Structure–Activity Relationships of C6-Uridine Derivatives Targeting *Plasmodia* Orotidine Monophosphate Decarboxylase†

Angelica M. Bello,[‡] Ewa Poduch,[‡] Yan Liu,[§] Lianhu Wei,[‡] Ian Crandall,[△,⊥] Xiaoyang Wang,[‡] Christopher Dyanand,[‡,#] Kevin C. Kain,[△,⊥] Emil F. Pai,[§,▽] and Lakshmi P. Kotra*[,‡,⊥,#,○]

Center for Molecular Design and Preformulations and Division of Cell and Molecular Biology, Toronto General Research Institute/University Health Network, MaRS/TMDT, 101 College Street, Toronto, Ontario M5G 1L7, Canada, Departments of Pharmaceutical Sciences and Chemistry, University of Toronto, Toronto, Ontario, Canada, Division of Cancer Genomics and Proteomics, Ontario Cancer Institute/ University Health Network, MaRS/TMDT, 101 College Street, Toronto, Ontario M5G 1L7, Canada, Departments of Biochemistry, Medical Biophysics, and Molecular Genetics, 1 King's College Circle, Toronto, Ontario M5S 1A8, Canada, Tropical Disease Unit, Division of Infectious Diseases, Department of Medicine, UHN-Toronto General Hospital and the University of Toronto and McLaughlin-Rotman Center/ UHN, McLaughlin Center for Molecular Medicine, University of Toronto, Toronto, Ontario, Canada, and Department of Chemistry and Biochemistry, The University of North Carolina at Greensboro, Greensboro, North Carolina 27412

Received August 28, 2007

Malaria, caused by *Plasmodia* parasites, has re-emerged as a major problem, imposing its fatal effects on human health, especially due to multidrug resistance. In *Plasmodia*, orotidine 5′-monophosphate decarboxylase (ODCase) is an essential enzyme for the de novo synthesis of uridine 5′-monophosphate. Impairing ODCase in these pathogens is a promising strategy to develop novel classes of therapeutics. Encouraged by our recent discovery that 6-iodo uridine is a potent inhibitor of *P. falciparum*, we investigated the structure–activity relationships of various C6 derivatives of UMP. 6-Cyano, 6-azido, 6-amino, 6-methyl, 6-*N*-methylamino, and 6-*N*,*N*-dimethylamino derivatives of uridine were evaluated against *P. falciparum*. The mononucleotides of 6-cyano, 6-azido, 6-amino, and 6-methyl uridine derivatives were studied as inhibitors of *plasmodial* ODCase. 6-Azidouridine 5′-monophosphate is a potent covalent inhibitor of *P. falciparum* ODCase. 6-Methyluridine exhibited weak antimalarial activity against *P. falciparum* 3D7 isolate. 6-*N*-Methylamino and 6-*N*,*N*-dimethylamino uridine derivatives exhibited moderate antimalarial activities.

Introduction

In the past few years, malaria attracted considerable attention in new drug discovery initiatives worldwide.[1] This infection is becoming a major burden on human health because drug-resistant strains of the malaria parasite are increasingly prevalent in most endemic areas, and current vaccine trials are not very encouraging.[2–4] While the majority of cases are now found in sub-Saharan Africa, it is predicted that global warming and demographic changes will lead to an increase in the distribution of clinical malaria cases in the Western world, including Europe and North America.[5] Existing drug pipelines, most of which are driven by public−private ventures, contain either derivatives or combinations of existing drugs.[1–3,5] Thus, the discovery of new classes of drugs against new targets is an important effort in the fight against malaria as well as against other emerging/ re-emerging infectious diseases.

Malaria is caused by the protozoa *Plasmodia*, and *P. falciparum* (*Pf*) is the most prevalent human parasite with approximately 70% of the human cases. It also causes the most lethal and severe form of malaria. Other human malaria parasites include *P. vivax* (*Pv*), *P. ovale*, and *P. malariae*. More than 95% of worldwide infections are caused by *Pf* and *Pv* alone.[6] *Plasmodia* species including *Pf* and *Pv* are dependent on their own de novo synthesis of pyrimidine nucleotides due to the absence of the salvage pathway in these parasites.[7–9] Therefore, if enzymes in this de novo pathway are inhibited in a plasmodial parasite, its only supply of pyrimidine nucleotides will be impaired. In humans, however, pyrimidine nucleotides are replenished via both the de novo and salvage pathways.[10] This makes inhibitors of de novo pyrimidine biosynthesis in *Plasmodia* quite attractive as novel therapeutic agents. In addition, the increasing prevalence of multidrug-resistant malaria parasites underscores the need for new drugs based on new molecular mechanisms and interacting with new targets, to complement the current therapeutic options.[5,6,11–15]

Orotidine 5′-monophosphate decarboxylase (ODCase[a]) plays a central role in the de novo synthesis of UMP, which in turn serves as the substrate for the synthesis of other pyrimidine nucleotides. ODCase catalyzes the decarboxylation of orotidine monophosphate (OMP, **1**) to uridine 5′-monophosphate (UMP, **2**, Chart 1).[16–18] This enzyme seems to be ubiquitous, present from bacteria, archaea, and parasites to higher species, including mammals and man, with viruses being the only exception. In the past three decades, ODCase has been investigated as a drug target, especially against various infectious diseases and

† PDB IDs for the coordinates of the complexes of ODCase with 6-iodo-UMP, 6-amino-UMP and 6-azido-UMP are 2QAF, 2Q8Z, and 3BAR, respectively.

* To whom correspondence should be addressed. Address: #418 New Science Building, The University of North Carolina at Greensboro, Dept. of Chemistry and Biochemistry, Greensboro, NC 27402. Tel.: (336) 334-9862. Fax: (416) 581-7621. E-mail: lpkotra@uncg.edu.

‡ Toronto General Research Institute/University Health Network.

§ Departments of Biochemistry, Medical Biophysics, and Molecular Genetics.

△ UHN-Toronto General Hospital and the University of Toronto and McLaughlin-Rotman Center/UHN.

⊥ McLaughlin Center for Molecular Medicine.

Departments of Pharmaceutical Sciences and Chemistry, University of Toronto.

▽ Ontario Cancer Institute/University Health Network.

○ The University of North Carolina at Greensboro.

[a] Abbreviations: ODCase, orotidine 5′-monophosphate decarboxylase; UMP, uridine 5′-monophosphate; OMP, orotidine 5′-monophosphate; BMP, barbiturate ribonucleoside 5′-monophosphate; TCEP HCl, tris(2-carboxyethyl)phosphine hydrochloride.

10.1021/jm7010673 CCC: $40.75
Published on Web 01/12/2008

Chart 1. Structures of ODCase Substrate and Inhibitors

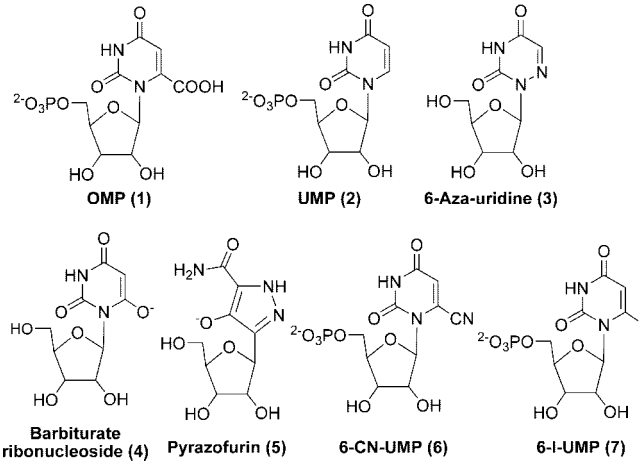

Chart 2. Structures of C6-Uridine Derivatives

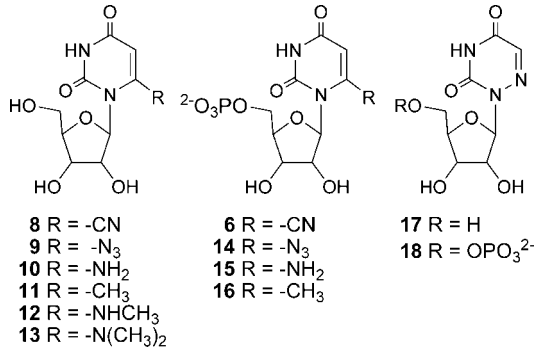

cancer.[19–21] The mononucleotide derivatives of 6-aza-uridine (**3**), barbiturate ribonucleoside (**4**), and pyrazofurin (**5**) are some of the inhibitors tested against ODCase (Chart 1).[20,22] The development of historic ODCase inhibitors as therapeutics did not gain much momentum due to their toxicities, lack of specificity, and the limited understanding of their mode of action.[20]

Our group recently reported novel inhibitors of ODCase that also interact via novel mechanisms. In this context, 6-cyano-uridine 5′-monophosphate (**6**, Chart 1) was investigated as a potential bioisosteric inhibitor of *Methanobacterium thermoautotrophicum* (*Mt*) ODCase using X-ray crystallography and enzymology.[23–25] ODCase catalyzed the unusual conversion of the chemically stable 6-cyano-uridine 5′-monophosphate (**6**) into barbiturate ribonucleoside 5′-monophosphate (BMP), with a half-life of 5 h, via what can be categorized as a "pseudo-hydrolysis" process.[23] In this unusual enzymatic conversion, no covalent interaction between the residues in the catalytic site of ODCase and the substrate was observed.[23,24] 6-Cyano-uridine 5′-monophosphate (**6**) also exhibited noncovalent, competitive inhibition of *Mt* ODCase activity with a K_i of 29 ± 2 μM.[24]

We also recently discovered the first covalent inhibitor of ODCase, 6-iodo-uridine 5′-monophosphate (6-iodo-UMP, **7**), and reported that its nucleoside analog exhibits potent antimalarial activities.[26] This compound **7** inhibited *Mt* ODCase irreversibly in a time-dependent fashion and 6-iodo-uridine, the nucleoside form of **7**, inhibited *Pf* in cell-based assays, with an IC_{50} of 4.4 ± 1.3 and 6.2 ± 0.7 μM (ItG and 3D7 isolates, respectively).[26] A cocrystal structure of the product of the suicide inhibitor 6-iodo-UMP (**7**), bound in the active site of *Mt* ODCase, clearly identified a covalent bond between Lys72 and the C6 atom on the pyrimidine ring, accompanied by the elimination of the 6-iodo moiety.[26] Prompted by these findings, we studied the structure–activity relationships of various C6-substituted uridine nucleotides as inhibitors of two *Plasmodia* ODCases and the potential of their nucleoside analogs as antimalarial agents. Here we present the design and the synthesis of several C6 derivatives of uridine and uridine 5′-monophosphate, inhibition profiles against *Plasmodia* ODCases, structural interactions of the novel inhibitors with ODCases and their antiplasmodial activities.

Experimental Section

General. All anhydrous reactions were performed under a nitrogen atmosphere. All solvents and reagents were obtained from commercial sources; anhydrous solvents were dried following standard procedures. Column chromatography was performed using silica gel (60 Å, 70–230 mesh). NMR spectra were recorded on a Varian spectrometer (300 and 400 MHz for ^{1}H, 75 and 100 MHz for ^{13}C, and 121.46 MHz for ^{31}P). The chemical shifts are reported in δ ppm using tetramethylsilane (TMS) as the reference for the ^{1}H NMR spectra and phosphoric acid as an external standard for the ^{31}P spectrum. All ODCase enzyme assays were performed at 55 or 37 °C using a VP-ITC microcalorimeter (MicroCal, Northampton, MA) using previously published procedures.[24] Mass spectra for the enzymes and the complexes were obtained in a Q-TOF mass spectrometer with MassLynx software for data analysis (Waters Micromass, Manchester, U.K.) at the Mass Spectrometry Facility, Advanced Protein Technology Centre, The Hospital for Sick Children, Toronto, Canada, and an AB/Sciex QStar mass spectrometer with an ESI source and on a an Agilent 1100 capillary LC attached (MDS Sciex, U.S.) at the Mass Spectrometry-AIMS Laboratory, Department of Chemistry, University of Toronto.

Synthesis. 6-Cyano-uridine (8) and 6-Cyano-uridine 5′-*O*-Monophosphate Ammonium Salt (6). These compounds were synthesized as reported earlier.[23]

6-Azido-uridine (9), 6-Azido-uridine 5′-*O*-Monophosphate Ammonium Salt (14) and 6-Amino-uridine 5′-*O*-Monophosphate Ammonium Salt (15). These compounds were synthesized as reported earlier.[24]

6-Amino-uridine (10). 6-Azido-uridine (**9**; 0.2 g, 0.7 mmol) was dissolved in 5 mL of 50% aqueous methanol and 10% Pd/C (5 mg) was added. The reaction mixture was stirred in the dark for 2 h under a hydrogen atmosphere at room temperature and atmospheric pressure. Then the reaction was filtered through a Celite pad and the solvent was evaporated to dryness to yield compound **10** as a light yellow solid in 94% yield (185 mg). UV (H_2O) λ_{max} = 271 nm; ϵ_{271} 18301; ^{1}H NMR (D_2O) δ 6.39 (d, J = 7.5 Hz, 1H), 4.83 (s, 1H), 4.61 (t, 6.9 Hz, 1H), 4.23 (dd, J = 3.3 and 6 Hz, 1H), 3.98 (m, 1H), 3.78 (m, 2H); ^{13}C NMR (D_2O) δ 166.2, 158.7, 152.9, 90.0, 86.9, 71.5, 71.2, 61.8, 30.7; HRMS (ESI, +ve) calcd for $C_9H_{13}N_3O_6Na^+$ (MNa^+), 282.0696; found, 282.0690.

6-Methyl-uridine (11). A stirred solution of LDA (0.6 mL, 1.2 mmol, 2.0 M solution in THF) in anhyd THF (2 mL) was treated with compound **19** (0.25 g, 0.63 mmol) dissolved in anhyd THF (1.5 mL) at −78 °C. After stirring for 1 h, methyl iodide (0.63 mmol) in dry THF (2 mL) was added and the mixture was stirred for an additional 5 h at −78 °C. The reaction was quenched with glacial AcOH (0.3 mL), then brought to room temperature and dissolved in ethyl acetate (25 mL). The organic layer was washed with saturated $NaHCO_3$ solution (10 mL) and brine (10 mL) and dried (Na_2SO_4). Evaporation of the solvent and purification of the crude by column chromatography (hexanes−ethyl acetate, 70:30) yielded the fully protected **20** as a foamy white solid.

A stirred aqueous suspension of compound **20** (300 mg, 0.73 mmol) was then treated with 50% aqueous TFA (3 mL) at 0 °C then brought to room temperature and stirred for an additional 2 h. Evaporation of solvent and purification of the crude by column chromatography (10–15% EtOH/$CHCl_3$) provided compound **11** as a white solid (169 mg, 90% yield). UV (H_2O) λ_{max} = 261 nm; ^{1}H NMR (D_2O) δ 5.78 (s, 1H), 5.68 (d, J = 3.2 Hz, 1H), 4.84 (dd,

J = 4 and 6 Hz, 1H), 4.41 (t, J = 6 Hz, 1H), 4.01–3.96 (m, 1H), 3.91 (dd, J = 3.2 and 12 Hz, 1H), 3.77 (dd, J = 6 and 12 Hz), 2.41 (s, 3H); HRMS (ESI, +ve) calcd for $C_{10}H_{15}N_3O_6Na^+$ (MNa^+), 296.0853; found, 296.0842.

6-*N*-Methylamino Uridine (12). 6-Iodo uridine[26] (**21**; 200 mg, 0.54 mmol) was dissolved in 20 mL of anhyd ethanol and then methylamine (0.60 mL, 2.16 mmol, soln 33 wt % in absolute EtOH) and triethylamine (1 mL) were added dropwise. The reaction mixture was stirred for 3 h at room temperature until compound **21** was consumed. The solvent was evaporated under vacuum and the product was purified by column chromatography ($CHCl_3$/MeOH, 9:1) to yield compound **12** as a pale yellow solid (73 mg, 50% yield). UV (H_2O) λ_{max} = 272 nm; ^{1}H NMR (CD_3OD) δ 7.89 (s, 1H), 6.45 (d, J = 7.6 Hz, 1H), 4.69 (s, 1H), 4.48 (dd, J = 6.4 and 7.6 Hz, 1H), 3.99 (m, 1H), 3.78 (m, 2H), 2.74 (s, 3H); HRMS (ESI, +ve) calcd for $C_{10}H_{15}N_3O_6Na^+$ (MNa^+), 296.0853; found, 296.0842.

6-*N*,*N*-Dimethylamino Uridine (13). Compound **13** was synthesized using the method described for compound **12**, starting from 6-iodo uridine **21** (100 mg, 0.27 mmol) and 0.55 mL of 2 M dimethylamine solution in THF (1.1 mmol) to yield compound **13** (70 mg, 90% yield). UV (H_2O) λ_{max} = 285 nm; ^{1}H NMR (CD_3OD) δ 5.70 (d, J = 4 Hz, 1H), 5.09 (s, 1H), 6.67 (dd, J = 4 and 6 Hz, 1H), 4.29 (t, J = 6 Hz, 1H), 3.86 (m, 1H), 3.79 (dd, J = 12 and 2.8 Hz, 1H), 3.67 (dd, 12 and 5.6 Hz, 1H), 2.85 (s, 6H); HRMS (ESI, +ve) calcd for $C_{11}H_{17}N_3O_6Na^+$ (MNa^+), 310.1009; found, 310.1012.

6-Methyl-uridine 5′-*O*-Monophosphate (16). A stirred solution of water (34 mg, 1.89 mmol) and $POCl_3$ (0.277 mL, 2.973 mmol) in anhyd acetonitrile (3 mL) was treated with pyridine (0.261 mL, 3.24 mmol) at 0 °C and stirred for 10 min. Compound **11** was added (185 mg, 0.675 mmol) and the mixture was stirred for an additional 5 h at the same temperature. The reaction mixture was quenched with 25 mL of cold water and the stirring was continued for an additional hour. The evaporation of the solvent and the purification of the crude by column chromatography (Dowex ion-exchange basic resin, 0.1 M formic acid) yielded compound **16** as a syrup. The mononucleotide derivative was then converted into the corresponding ammonium salt by neutralization with 0.5 M NH_4OH solution at 0 °C and lyophilized to yield the corresponding ammonium salt as a white powder (140 mg, 56% yield). UV (H_2O) λ_{max} = 260 nm; ϵ_{260} (H_2O) = 2271; ^{1}H NMR (D_2O) δ ppm 5.75 (s, 1H), 5.67 (d, J = 6 Hz, 1H), 4.63 (dd, J = 6, 7 Hz, 1H), 4.44 (t, J = 7 Hz, 1H), 4.14–4.02 (m, 2H), 4.00–3.92 (m, 1H), 2.39 (s, 3H); HRMS (ESI, positive) calcd for $C_{10}H_{15}N_2O_9PH^+$ (MH^+), 339.0587; found, 339.0587.

Enzymology. Cloning, Expression, and Purification of ODCases. The ODCase enzymes from *Mt* and *Pf* were produced as described earlier.[26,27]

General Methods for Enzyme Assays. All enzymatic assays were performed on a VP-ITC calorimeter (MicroCal, MA). Tris buffer (50 mM, pH 7.5) was prepared using Millipore water and filtered through a membrane (0.45 μm) to remove any fine particles. The substrate stock solution and the inhibitor solutions were prepared using 50 mM Tris and diluted as required. All solutions were degassed for 5 min using a Thermovac vacuum degasser (MicroCal, MA). The control reaction contained no inhibitor. The enzyme activity was determined either at 37 or 55 °C for *Pf* and *Mt* ODCases, respectively. The assays were performed using the single injection method, where the ligand is injected into the reaction cell containing the enzyme solution. The inhibitor was either injected together with the substrate into the enzyme solution or mixed with the enzyme. In the second scenario, the reaction was initiated by the addition of substrate only.

***Mt* ODCase. Reversible Inhibition Studies.** The final concentration of the enzyme in all assays was 20 nM and that of the substrate was 40 μM. The inhibition of *Mt* ODCase by 6-methyl-UMP (**16**) was recorded in the presence of 50, 150, 350, and 500 μM of the inhibitor. The enzyme was mixed with the inhibitor in 50 mM Tris and 1 mM DTT, and the reaction was initiated by the addition of the substrate. The reversible inhibition by 6-azido-UMP (**14**) was determined after the coinjection of the substrate and the inhibitor. The concentrations of 6-azido-UMP (**14**) in the assay samples were 0.25, 0.50, and 1.0 μM.

Irreversible Inhibition Studies. The *Mt* ODCase was incubated in the absence and presence of an inhibitor (for example, 6-azido-UMP, **14**) for up to 48 h at room temperature. The control reaction contained 20 μM ODCase in 50 mM Tris (pH 7.5), 20 mM DTT, and 40 mM NaCl. The inhibition reactions contained 20, 40, or 60 mM of the inhibitor. The remaining enzyme activity was measured after 0.3, 1, 2, 4, 8, 12, 24, and 48 h after the initiation of the enzyme reaction. A single injection of 5 mM substrate (11.4 μL) provided the initial concentration of the substrate OMP in the reaction cell at 40 μM. The inactivation of ODCase by 6-azido-UMP without incubation was also determined following a coinjection of the substrate and the inhibitor into the enzyme solution. Enzyme samples were prepared in degassed 50 mM Tris buffer containing 1 mM DTT. The final enzyme concentration was 20 nM. Inhibitor was added to the sample cell in a single 22.8 μL injection together with the substrate, and the enzyme activity was recorded. The final substrate concentration in the 1.3 mL cell was 40 μM. The inhibitor concentration after a single injection was 0, 0.25, 0.50, 1, 3, or 6 μM.

***Pf* ODCase.** *Pf* ODCase stock was prepared in 50 mM Tris (pH 7.5), 10 mM DTT, and 20 mM NaCl and was incubated overnight at room temperature. The reversible inhibition of ODCase was assayed after the dilution of a 2.5 μL aliquot of the concentrated enzyme and an appropriate volume of concentrated inhibitor in 50 mM Tris, containing 1 mM DTT to a final volume of 2.5 mL. The enzyme activity of *Pf* ODCase was measured after a single injection of the substrate.

Reversible Inhibition Studies. The inhibition of *Pf* ODCase by 6-cyano-UMP (**6**), 6-aza-UMP (**18**), and 6-methyl-UMP (**16**) was evaluated using competitive inhibition assays. The mixture of the enzyme and the inhibitor was prepared from the stock solutions and the samples were immediately transferred into the calorimeter cell. The concentration of the enzyme was 60 nM for the inhibition assays using 6-cyano-UMP (**6**) and 6-aza-UMP (**18**), and was 100 nM with 6-methyl-UMP (**16**). The final concentrations of the inhibitor in the reaction cell were 25, 50, and 75 μM for 6-cyano-UMP (**6**) and 1, 2, 3, 5, 7.5, and 10 μM for 6-aza-UMP (**18**). In the case of 6-methyl-UMP (**16**), the concentrations of the inhibitor in the sample cell were 20, 150, and 250 μM. The substrate concentration was 12 μM after a single injection of OMP. The reversible inhibition assays with 6-amino-UMP (**15**) and 6-azido-UMP (**14**) were conducted with 30 nM *Pf* ODCase. The final substrate concentration was 10 μM. The enzyme was exposed to the final concentrations of 1, 2.5, 3.5, and 5 μM of 6-amino-UMP (**15**) or 2, 5, 10, and 15 μM of 6-azido-UMP (**14**).

Time-Dependent Inhibition Studies. *Pf* ODCase (50 μM) was incubated in the presence of 12.5, 25.0, and 50.0 mM of 6-cyano-UMP (6). All samples were prepared in 50 mM Tris (pH 7.5), 20 mM DTT, and 40 mM NaCl and incubated at room temperature. The control reaction contained no inhibitor. The samples were incubated for 0, 0.3, 1, 2, 4, 8, 12, 24, and 48 h. The remaining enzyme activity at each time point was measured by using 2.5 μL aliquots of the reaction mixture, which were diluted 1000-fold with 50 mM Tris containing 1 mM DTT. The final substrate concentration was 12 μM.

The inhibition of ODCase due to 6-azido-UMP (**14**) was monitored in a time-dependent assay. The control reaction contained 30 μM of the enzyme in 50 mM Tris (pH 7.5), 20 mM DTT, and 83 mM NaCl. The incubation samples contained 30 μM *Pf* ODCase and 0.4, 1.0, 5.0, or 10.0 mM of **14** in 50 mM Tris (pH 7.5), 20 mM DTT, and 83 mM NaCl. The samples were incubated at room temperature for 0.5, 1, 2, 4, 8, 12, 24, and 48 h. At each incubation time point, 2.5 μL aliquots of the control and reaction samples were removed from the incubation mixtures and diluted to 2.5 mL with 50 mM Tris buffer containing 1 mM DTT. The remaining activity of *Pf* ODCase in the presence of the inhibitor was measured after a single 5 μL injection of 2.85 mM OMP into the sample cell. The final substrate concentration was 10 μM.

***Pv* ODCase. Competitive Inhibition Assay.** The enzyme was mixed with various concentrations of the inhibitor in 50 mM Tris containing 1 mM DTT to a final volume of 2.5 mL. The activity of *Pv* ODCase (50 nM) was monitored in the presence of 40, 75, and 150 μM of 6-cyano-UMP (6). The inhibition assay for 6-methyl-UMP (16) was performed using 50, 150, and 250 μM inhibitor and 70 nM ODCase enzyme. The final concentration of the substrate was 12 μM in the reaction cell after a single injection of OMP into the calorimetric sample cell.

Time-Dependent Assay. The time-dependent inhibition of *Pv* ODCase was studied at 25 °C. The reaction and the control samples contained *Pv* ODCase (50 μM) in 50 mM Tris (pH 8.0), 20 mM DTT, and 10 mM NaCl. The initial concentrations of the inhibitor (added at $t = 0$) were 37.5, 50, and 75 mM, corresponding to 750-, 1000-, and 1500-fold molar excess of the inhibitor (6-cyano-UMP, **6**). Small aliquots (2.5 μL) were withdrawn from the incubation samples and diluted to 2.5 mL with the reaction buffer (50 mM Tris, 1 mM DTT, pH 8). The enzyme activity was measured in the inhibition reaction sample and the control after 1, 2, 4, 8, 12, 24, 36, and 48 h of incubation. The enzyme activity was recorded after a single injection of the substrate into the sample solution. A 6 μL injection of OMP (2.85 mM) gave a final substrate concentration of 12 μM.

Mass Spectral Analyses. The control reaction with *Pf* ODCase (300 μM) was prepared in 20 mM Tris buffer (pH 8) containing 10 mM DTT and 20 mM NaCl. Samples contained 300 μM of the enzyme, 6 mM 6-azido-UMP (**14**), 20 mM Tris (pH 8), 10 mM DTT, and 20 mM NaCl. Mass spectral analyses for samples at $t =$ 0 s were conducted immediately before mixing the inhibitor with the enzyme. The control sample and the mixture of *Pf* ODCase with 6-azido-UMP (**14**) were incubated at room temperature in the dark for 72 h, and the mass spectral analyses were repeated.

Data Analyses. The data were analyzed using the "Enzyme Assay" module available from the Origin 7.0 data analysis package. First the raw data were adjusted for the instrument response time. The baselines were set to zero using the "Baseline" function, and the data were truncated to remove the initial baseline, dilution heat, and the final baseline. The remaining data representing the enzymatic decarboxylation of OMP in the absence or in the presence of a reversible inhibitor were transformed into Michaelis–Menten plots by fitting them to the equation

$$v = \frac{k_{cat}[E][S]}{K_M + [S]} \quad (1)$$

The curves were averaged for each set of samples. Several data points representing the reaction rate at specific substrate concentrations were extracted from the Michaelis–Menten curves and were used to generate a Dixon plot.[24,28] The inhibition constant K_i was established for each inhibitor as the intersection point on the *x*-axis from the plots of $[I]$ vs rate^{-1}. For the time-dependent inhibition of ODCase, the remaining enzyme activity in the incubation sample was determined as a percentage of the control at each time point.

The half-time of the enzyme inhibition for the assay with 6-cyano-UMP was calculated using the equation for a single exponential decay.

$$A = A_0 e^{-kt} \quad (2)$$

where A represents 50% of enzyme activity, A_0 is the initial activity at time 0 (extrapolated from the nonlinear least-squares fitting of the data to eq 2, k is the rate constant, and t represents the time required to inhibit 50% of the enzyme activity.

Time-Dependent Inhibition. The remaining enzyme activity was determined for both *Mt* and *Pf* ODCase enzymes using 6-azido-UMP (**14**) as a percentage of the activity of the control. To determine the inactivation of *Mt* ODCase after the coinjection of substrate and inhibitor, k_{obs} was first computed from each progress curve. The value (Power, μcal/sec) at each inflection point was normalized by setting the inflection point value to zero. The data representing the change in power over time were fitted to the following equation to calculate k_{obs}

$$[P] = \frac{v_i}{k_{obs}}[1 - \exp(-k_{obs}t)] \quad (3)$$

where $[P]$ represents the product concentration, v_i is the initial reaction rate, and t is the time. The calculated k_{obs} and the inhibitor concentrations $[I]$ were used to calculate the inactivation constant K_I and the rate of inactivation k_{inact} from the equation

$$k_{obs} = \frac{k_{inact}[I]}{K_I + [I]} \quad (4)$$

The kinetic parameters for the inactivation of *Pf* ODCase were derived using the data points for up to 4 h of incubation with the inhibitor. The remaining enzyme activity was calculated for each incubation time point as a percentage of the control sample. The natural logarithm of % enzyme activity was plotted against time to obtain the observed rate of enzyme inactivation (k_{obs}) at each inhibitor concentration. Then k_{obs} and inhibitor concentrations were fitted to the eq 4 to calculate K_I and k_{inact}.

***P. falciparum* and CHO Cell Inhibition Assays.** *P. falciparum* cultures were grown in O^+ blood obtained by venipuncture of volunteers. The cultures of the laboratory line ItG were maintained by the method of Trager and Jensen[29] using RPMI 1640 supplemented with 10% human serum (a kind gift obtained under ethical consent from the Chemo Day Care Department, Princess Margaret Hospital, Toronto, Canada) and 50 μM hypoxanthine (RPMI-A). The assays comparing the antiplasmodial activities of the inhibitors were performed using the SYBR-Green method.[30] Briefly, the inhibitors were dissolved in DMSO to achieve a concentration of 10 mg/mL. RPMI-A (50 μL) was added to each well in a 96-well plate before 40 μL of RPMI-A and 10 μL of the inhibitor solution were added to the first well, the contents of the well were mixed, 50 μL were removed and added to the next well in the series, and the process was repeated until the next-to-last well was reached. This produced a plate with a series of 2-fold dilutions across it, except for the last well in the series, which contained RPMI-A alone. The parasite culture (50 μL, 2% hematocrit, 2% parasitemia) was added to each well and the plates were incubated at 37 °C in 95% N_2, 3% CO_2, and 2% O_2 for 48 h. Relative fluorescence was determined using a Fluostar Optima plate reader (BMG Labtech, Offenburg, Germany). The IC_{50} values of individual compounds were determined using a nonlinear regression analysis of the data using the computer program SigmaPlot (Jandel Scientific). The IC_{50} values represent the mean ± SD, $n = 4$.

The CHO cells (ATCC, Manassas, VA) were grown in RPMI-1640 supplemented with 10% fetal calf serum (Sigma, St. Louis, MO), 25 mM HEPES, and gentamicin (RPMI-10). The cells were seeded in 96-well plates and were grown to 50% confluency in 100 μL of RPMI-10 per well prior to the addition of either DMSO alone or a test compound dissolved in DMSO to a concentration of 10 mg/mL. The inhibitor solutions were prepared by adding 90 μL of RPMI-10 mixed with 10 μL of inhibitor solution to the first well in the series, mixing, transferring 100 μL to the next well, and repeating until the next-to-last well was reached. After 48 h, the media in the wells were discarded, 100 μL of 10 mg/mL of 3-[4,5-dimethylthiazol-2-yl]-2,5-diphenyltetrazolium bromide (MTT, Sigma, St. Louis, MO) in RPMI-10 was added, and the plates were incubated for an additional hour. The viability of the cells was determined by removing the media followed by the addition of 100 μL of DMSO and reading the absorbance at 650 nm.[31] The IC_{50} values of individual compounds were determined, applying a nonlinear regression analysis of the dose–response curve using the computer program SigmaPlot (Jandel Scientific).

Crystallographic Analyses. All *Pf* ODCase concentrations were determined using a BioRAD protein assay kit and BSA as a standard. ODCase protein was dissolved in 20 mM Tris (pH 8.5), 10 mM NaCl, and 1 mM TCEP-HCl. *Pf* ODCase complex crystals were grown in hanging drops using ~30% PEG1000, pH 7.0–9.0, as the main precipitant. To obtain larger single crystals of the enzyme complexes, microseeding was performed the following day. All crystals grew in space group $P2_12_12$, with unit cell dimensions

Table 1. Inhibition Kinetics of C6-Substituted UMP Derivatives against ODCases from *P. falciparum* (*Pf*), *P. vivax* (*Pv*), and *M. thermoautotrophicum* (*Mt*)

cmpd	*Mt* K_i (μM)	*Pf* K_i (μM)	*Pv* K_i (μM)
6-CN-UMP (**6**)	29 ± 2	26 ± 2	62 ± 5
6-N_3-UMP (**14**)	0.19 ± 0.01	2.0 ± 0.1	ND
6-NH_2-UMP (**15**)	0.84 ± 0.025	2.1	ND
6-Me-UMP (**16**)	134 ± 5	34.1 ± 0.4	22.4 ± 0.7
6-Aza-UMP (**18**)	12.4 ± 0.7	1.1 ± 0.03	ND
Time-Dependent Inactivation of *Pf* ODCase			
6-N_3-UMP (**14**) (K_I and k_{inact})	0.63 ± 0.11 μM 61.2 h^{-1}	7.3 ± 0.4 μM 0.35 h^{-1}	ND

deviating less than 1% from $a = 80.8$ Å, $b = 83.1$ Å, and $c = 90.0$ Å. For data collection, the crystals were cryo-protected by Parotone-N oil before flash-freezing in a stream of boiling nitrogen. Diffraction data for the crystals of *Pf* ODCase cocrystallized with both 6-amino-UMP (**15**) and 6-iodo-UMP (**7**) were collected at 100 K and $\lambda = 0.9002$ Å on beamline 14BM-C BioCARS, APS, and those for the 6-azido-UMP (**14**) exposed crystals at 100 K and $\lambda = 0.97934$ Å on beamline 08ID-1 at the Canadian Macromolecular Crystallography Facility, Canadian Light Source, Inc. Data were reduced and scaled using HKL2000.[32] Data collection statistics are given in Table 2. The structures of all complexes were determined using molecular replacement techniques with the help of the program package MOLPREP;[33] subsequent refinements were done with Refmac-5.2[34] and model building used COOT.[35] The refinement statistics are also given in Table 2. Atomic coordinates and structure factors have been deposited into the Protein Data Bank (PDB IDs: 2QAF, 2Q8Z, and 3BAR).

Computer Modeling. Computer modeling was performed using the SYBYL suite of software on an SGI workstation at the Center for Molecular Design and Preformulations at University Health Network, Toronto.[36] The structure of the complex of 6-methyl-UMP (**16**) and *Pf* ODCase was modeled by mutating the 6-amino group to a 6-methyl group in the X-ray crystal structure of the complex of 6-amino-UMP (**15**) bound to *Pf* ODCase. Similarly, *Pf* ODCase complexes with 6-methylamino-UMP or 6-dimethylamino-UMP structures were modeled by mutating one or two hydrogen atoms on the 6-amino group of compound **15** with one or two methyl groups, respectively. Conformations of the *N*-methylamino and *N*,*N*-dimethylamino moieties were positioned in the best possible orientation within the binding site with minimal steric crowding.

Results and Discussion

All nucleoside and mononucleotide derivatives (**6**, **8**–**13**, and **14**−**16**) were synthesized from the fully protected uridine derivative **19**. The 6-cyano derivatives **6** and **8** were synthesized according to a previous report.[23] 6-Amino-uridine (**10**) was synthesized by catalytic hydrogenation of 6-azido-uridine (**9**) at room temperature for 3 h (Scheme 1A).[24] 6-Amino-UMP (**15**) was similarly obtained by the reduction of 6-azido-UMP (**14**).[24] Compounds **12** and **13** were synthesized by the displacement of the iodo moiety from 6-iodo-uridine (**23**) with methylamine and dimethylamine, respectively, in ethanol at room temperature (Scheme 1B). Our attempts to phosphorylate 6-*N*-methylamino-uridine (**12**) and 6-*N*,*N*-dimethylamino-uridine (**13**) were not successful and products of decomposition were observed. 6-Methyl-UMP (**16**) was synthesized according to Scheme 1C. The methyl group at the C6 position was introduced onto the fully protected uridine **19** first by treating with lithium diisopropylamide followed by methyl iodide. The deprotection of **20** with trifluoroacetic acid yielded 6-methyl-uridine (**11**), followed by phosporylation with phosphorus oxychloride afforded the mononucleotide **16**. Compound **16** was transformed into its ammonium salt by neutralization with 0.5 M NH_4OH solution.

These C6-substituted UMP derivatives were investigated as antiplasmodial agents following the discovery that C6 substitutions on UMP exhibit potent ODCase inhibition and confer potent antiplasmodial activities.[24,26] Previously, compound **6** exhibited interesting activities against *Mt* ODCase and was converted into BMP by this enzyme. Additionally, 6-cyano-UMP (**6**) inhibited this enzyme competitively with moderate potency.[24] Thus, compound **6** was of interest for evaluation against *Pf* and *Pv* ODCases. Compound **14** carries an azido moiety at the C6 position, a substitution with one atom "longer" than the nitrile moiety and is linear in shape. It is also a reasonably good leaving group similar to the iodo moiety. The 6-methyl derivative **16** addressed the question what effect a small hydrophobic moiety at this position has on ODCase inhibition and antiplasmodial activity.

First, all nucleotide derivatives **6**, **14**−**16**, and **18** were first evaluated for their inhibitory potential against *Pf* ODCase, followed by the *Pv* and *Mt* enzymes. 6-Aza-UMP (**18**), which is a classic inhibitor of ODCases, provided excellent comparative values for *Pf* ODCase. While compound **18** was a moderate inhibitor of *Mt* ODCase, with a K_i of 12.4 ± 0.7 μM, when challenged with *Pf* ODCase, it exhibited stronger inhibition potential (K_i = 1.1 ± 0.03 μM). However, this is still approximately 15-fold less potent than its effect on the yeast enzyme.[24] 6-Cyano-UMP (**6**) showed a typical competitive inhibition pattern, as was observed with *Mt* ODCase in earlier studies.[24] However, when 6-cyano-UMP (**6**) was incubated with *Pf* ODCase for several hours, it was transformed into BMP (**4**), as had been observed with *Mt* ODCase (Figure 3B).[23] The time required for the enzyme to lose 50% of its activity was 7, 5, and 3 h in the presence of 12.5, 25, and 50 mM of 6-cyano-UMP, and such loss of activity is due to the conversion of 6-cyano-UMP into BMP. The inhibition constant (K_i) against *Pf* ODCase for **6** in the competitive assay was 29 ± 2 μM, which is very close to that with *Mt* ODCase (26 ± 2 μM; Figure 3A and Table 1). However, compound **6** exhibited a slightly weaker inhibition against *Pv* ODCase, with a K_i of 62 ± 5 μM (Table 1). 6-Methyl-UMP (**17**) is a competitive inhibitor with moderate potency against *Pf* and *Pv* ODCases (K_i = 34.1 ± 0.4 and 22.4 ± 0.7 μM, respectively; Figure 3C).

6-Amino-UMP (**15**) and 6-azido-UMP (**14**) exhibited quite interesting inhibition profiles (Figure 3D, and E, respectively). Compound **15** inhibited *Mt* ODCase competitively, with a K_i of 840 ± 25 nM. This compound, however, showed slightly less potency against *Pf* ODCase, with a K_i of approximately 2.1 ± 0.0 μM (Table 1). Potent inhibition due to 6-amino-UMP (**15**) is perhaps expected based on the well-characterized inhibition pattern of ODCases by BMP, which carries a hydroxyl moiety at the C6 position.[24]

We earlier reported 6-iodo-UMP (**7**) as the first covalent inhibitor of ODCase and showed that an irreversible enzyme complex with the inhibitor was observed using mass spectrometry (*Pf* ODCase), enzymology (*Pf* ODCase), and X-ray crystallography (*Mt* ODCase).[26] In the present studies, 6-azido-UMP (**14**) was identified as another covalent inhibitor for ODCase, exhibiting a potent, covalent inhibition of the enzyme (Figures 1C,D, 3E,F, and 4B). When initial rates were monitored, compound **14** inhibited *Mt* and *Pf* ODCases, with K_i = 0.19 ± 0.01 and 2.0 ± 0.1 μM, respectively. In a time-dependent assay, 6-azido-UMP (**14**) inactivated *Mt* and *Pf* ODCases, with an equilibrium inhibition constant (K_I) of 628 ± 110 nM and

Table 2. Data Collection and Refinement Statistics for the X-ray Crystal Structures of the Complexes of ODCase with the Inhibitors **7**, **14**, and **15**[a]

	Pf ODCase + 6-I-UMP (**7**)	*Pf* ODCase + 6-N_3-UMP (**14**)	*Pf* ODCase + 6-NH_2-UMP (**15**)
	Diffraction Data		
resolution (Å)	1.95 (1.98–1.95)	1.90 (1.97–1.90)	1.80 (1.83–1.80)
measured reflections (*n*)	203475	241881	266845
unique reflections (*n*)	43303	46532	54102
completeness (%)	95.6 (98.0)	95.5 (97.9)	94.6 (97.0)
R_{sym} (%)	10.2 (49.2)	8.5 (45.9)	9.7 (43.5)
space group	$P2_12_12$	$P2_12_12$	$P2_12_12$
molecules in asymmetric unit (*n*)	2	2	2
	Refinement Statistics		
resolution (Å)	28.30–1.95 (2.00–1.95)	26.0–1.90 (1.95–1.90)	24.57–1.80 (1.84–1.80)
protein atoms (*n*)	5461	5670	5478
water molecules (*n*)	252	257	247
reflections used for R_{free} (*n*)	2191 (152)	2357 (167)	2752 (366)
R_{work} (%)	17.13 (18.7)	17.2 (19.6)	16.7 (19.1)
R_{free} (%)	22.51 (24.7)	21.9 (25.4)	21.2 (27.6)
root mean square deviation bond length (Å)	0.010	0.010	0.010
root mean square deviation bond angle (°)	1.665	1.487	1.500
avg B-factor (Å^2)	19.84	22.1	22.27

[a] Numbers in brackets are for the highest resolution shells. $R_{sym} = S|I - \langle I \rangle|/SI$, where I is the observed intensity and $\langle I \rangle$ is the average intensity from multiple observations of symmetry-related reflections.

Scheme 1. Synthesis of ODCase Inhibitors[a]

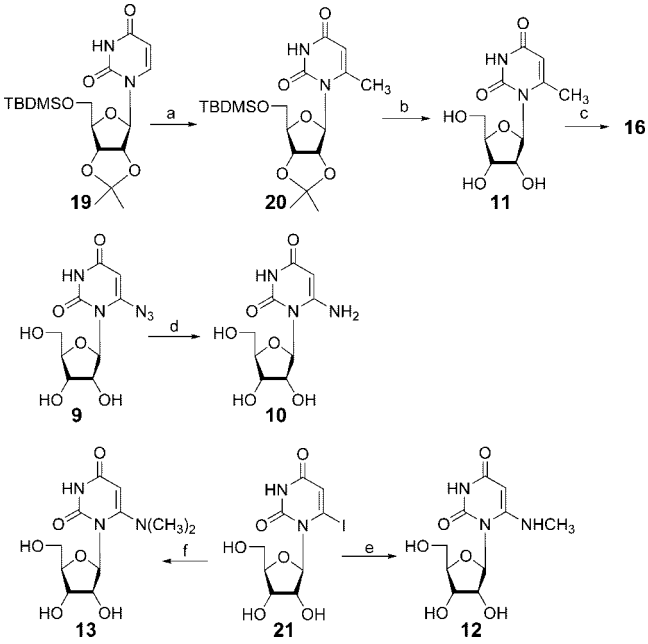

[a] Reagents and conditions: (a) LDA/THF, CH_3I, −78 °C; (b) 50% TFA/H_2O, 0–25 °C; (c) $POCl_3$, Py, H_2O, CH_3CN, 0 °C; (d) H_2, Pd/C, MeOH, rt; (e) CH_3NH_2, EtOH, rt; (f) $NH(CH_3)_2$, EtOH, rt.

7.3 ± 0.4 μM, respectively. The first-order rates of inactivation (k_{inact}) were 61.2 h^{-1} and 0.35 h^{-1}, respectively. 6-Iodo-UMP (**7**) inhibited *Pf* ODCase with a second-order rate constant (k_{obs}/[*I*]) of 680000 M^{-1}sec^{-1}. On the other hand, when *Pf* ODCase was challenged with 6-azido-UMP (**14**), the second-order rate constant (k_{inact}/K_I) for the inactivation of the enzyme was 13.2 M^{-1}sec^{-1}, indicating that fewer molecules of 6-azido-UMP were forming a covalent bond at the active site Lys138 than had been observed with **7**.

High-resolution X-ray crystallography experiments with the inhibitors **7** and **14** revealed in detail the interactions of these inhibitors with the active site of ODCase. Crystal structures of *Pf* ODCase incubated with 6-iodo-UMP (**7**) and 6-azido-UMP (**14**) were almost identical, both revealing covalent enzyme–inhibitor complexes (Figure 1 and Table 2). The crystal structure (1.95 Å resolution) of *Pf* ODCase incubated with 6-iodo-UMP (**7**) showed that the iodo moiety was lost and a covalent bond was formed between Nϵ of Lys138 and C6 of the inhibitor, as was previously observed with *Mt* ODCase. The same result was obtained when 6-azido-UMP (**14**) was used instead; again, the X-ray crystal structure (1.90 Å resolution) confirmed the covalent bond formation (Figure 1C,D). In both cases, the pyrimidine moiety engages in three strong hydrogen bonding interactions with the ODCase binding site, specifically between Nϵ of Gln269 and O2 of the ligand, the hydroxyl moiety of Thr195 and N3 of the ligand, and from the backbone NH of Thr195 to O4 of the ligand (bond lengths of 2.83, 2.75, and 2.92 Å, respectively). This pattern is similar to that found with other noncovalently bound ligands.[23,27] The 5′-monophosphate portion of the ligand, which is responsible for most of the binding energy, interacts via five tightly bound water molecules and the critical Arg294 residue in the *Pf* ODCase binding site. The ribosyl moiety is held via a number of interactions, including residues from the second subunit of the dimer. The 2′-hydroxyl moiety shares three hydrogen bonds with the side chains of Asp141B (Oγ), Thr145B (Oγ), and Asn104 (Nϵ; bond lengths of 2.44, 2.83, and 2.80 Å, respectively); the 3′-hydroxyl moiety interacts with the side chains of Lys102 (Nϵ), Asp23 (Oγ), and Asn104 (Oγ; bond lengths of 3.45, 2.76 and 2.94, Å, respectively) via hydrogen bonds (Figure 1A,C).

Mass spectral analyses for the reactions of 6-iodo-UMP (**7**) and 6-azido-UMP (**14**) with *Pf* ODCase revealed that identical covalent adducts are formed as expected (Figure 4). Thus, the reaction between **7** and *Pf* ODCase showed a peak at 40042 daltons (Figure 4A, peak 1), which is equivalent to the sum of the average mass of *Pf* ODCase (39720 dalton, inset in Figure 4A, peak 2) and **7** without the iodo moiety (323 dalton). This resulting mass additionally reflects the loss of two protons from the Lys138 residue, which is engaged in a covalent bond with C6 of the ligand. These results parallel those obtained with *Mt* ODCase.[26] A separate study using 6-azido-UMP **14** and *Pf* ODCase generated an identical adduct with an average mass of 40042 dalton (Figure 4B, Peak 4), which is equivalent to the major adduct observed after the reaction between 6-iodo-UMP and *Pf* ODCase.

The three-dimensional (3D) structure (1.8 Å resolution) of the complex between 6-amino-UMP (**15**) and *Pf* ODCase confirmed that the complementary interactions at the C6 position

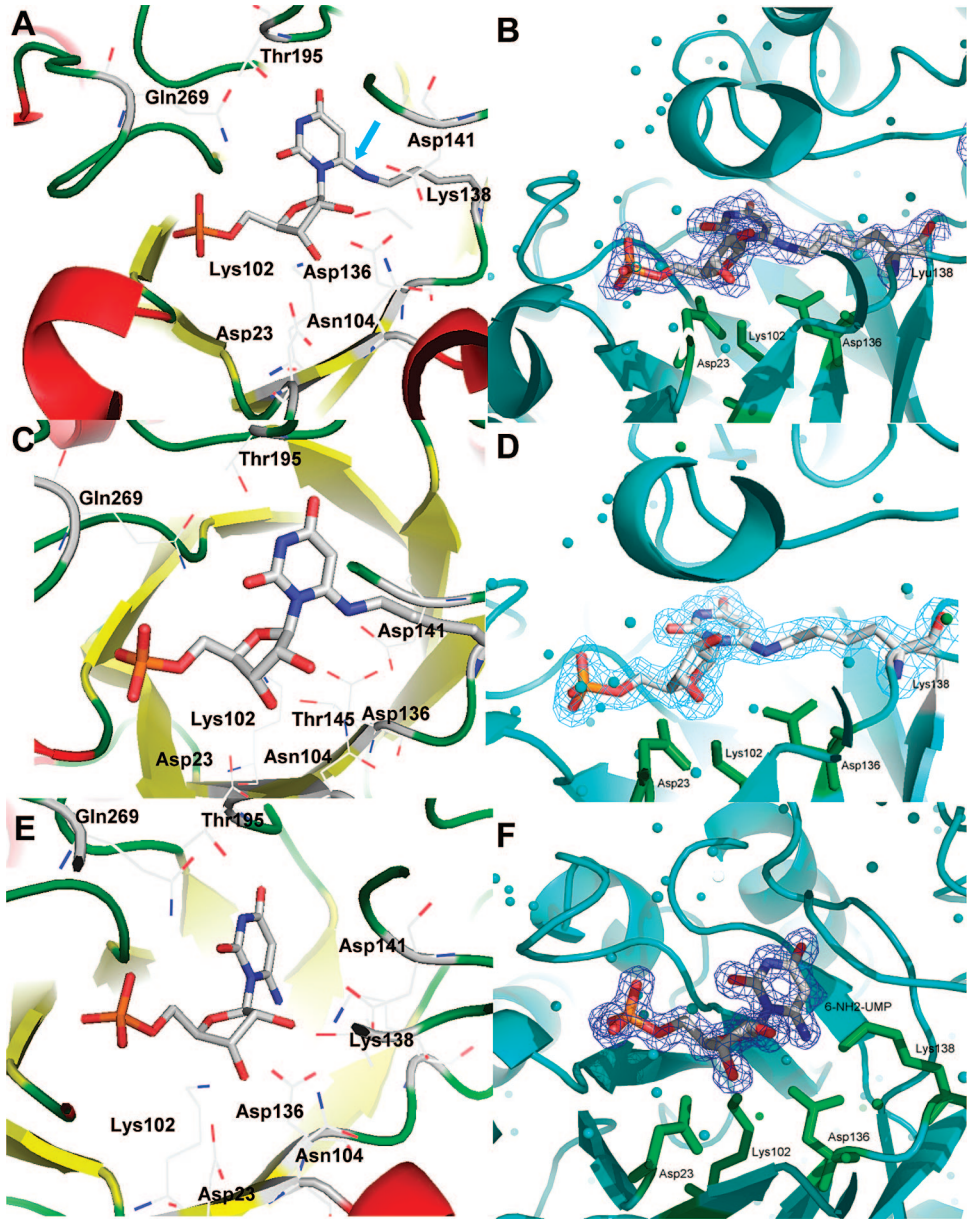

Figure 1. X-ray crystal structures of the complexes generated by incubating *Pf* ODCase with 6-iodo-UMP (A and B), 6-azido-UMP (C and D), and 6-amino-UMP (E and F). Panels A and C depict the covalent ligand resulting from 6-iodo-UMP and 6-azido-UMP (**7** and **14**, respectively), panel E shows 6-amino UMP (**15**) bound to the active site of ODCase; inhibitor molecules and the covalently bound residue Lys138 (in A and C) are shown in capped-stick representation and the other protein residues are shown in line representation. Covalent bonds between the enzyme and the inhibitors are highlighted by blue arrows. Panels B, D, and F depict the electron densities ($2F_o - F_c$) corresponding to the inhibitor molecules, displayed at 1σ level. Enzyme backbones are rendered according to their secondary structures and the ligands are shown in capped-stick representation.

on the pyrimidine moiety are necessary for potent inhibition (Figure 1E,F). The hydrogen bonding interactions with the pyrimidine moiety at positions O2, N3, and O4 were similar to those observed with 6-iodo-UMP (Figure 1E). The charged 5′-monophosphate moiety exhibited the well-characterized interactions with five water molecules and the Arg294 residue. The ribosyl moiety was held in a conformation similar to that with **7** as a result of (i) the interactions of the 2′-hydroxyl moiety with the side chains of Asp141B, Thr145B, and Asn104 and (ii) the hydrogen bonding interactions of the 3′-hydroxyl moiety with the side chains of Lys102, Asp23, and Asn104. Interestingly, the 6-amino moiety in **15** is in close proximity to an active site water molecule (N_7-HOH265 = 2.58 Å) and the Nϵ moiety of Lys138 (N_7-Nϵ of Lys138 = 2.37 Å). It also interacts with the side chain of Asp136 (Figure 1E). These strong interactions of the 6-amino moiety (N_7) in compound **15** are contributing to the potent inhibition of *Pf* ODCase.

Structures of the complexes of 6-methylamino-UMP, 6-dimethylamino-UMP, and 6-methyl-UMP (**16**) with *Pf* ODCase were modeled based on the structure of the complex of *Pf* ODCase and 6-amino-UMP to shed light on the potential interactions between these compounds and the enzyme active site. Although 6-*N*-methylamino-UMP and 6-*N*,*N*-dimethylamino-UMP could not be synthesized, we were nevertheless interested in modeling these compounds in the binding site of ODCase because the corresponding nucleoside derivatives (**12** and **13**) exhibited weak antimalarial activities (Table 3). Most likely, compounds **12** and **13** were phosphorylated by kinases in vivo, transforming them into the inhibitors of *Pf* ODCase,

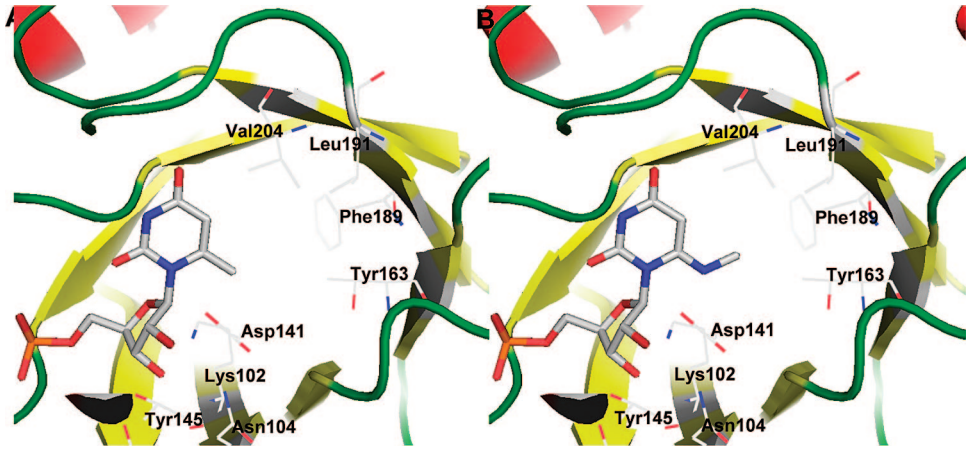

Figure 2. Computational models of the 3D structures of the complexes of *Pf* ODCase with 6-methyl-UMP, **16** (Panel A), and 6-*N*-methylamino-UMP (Panel B).

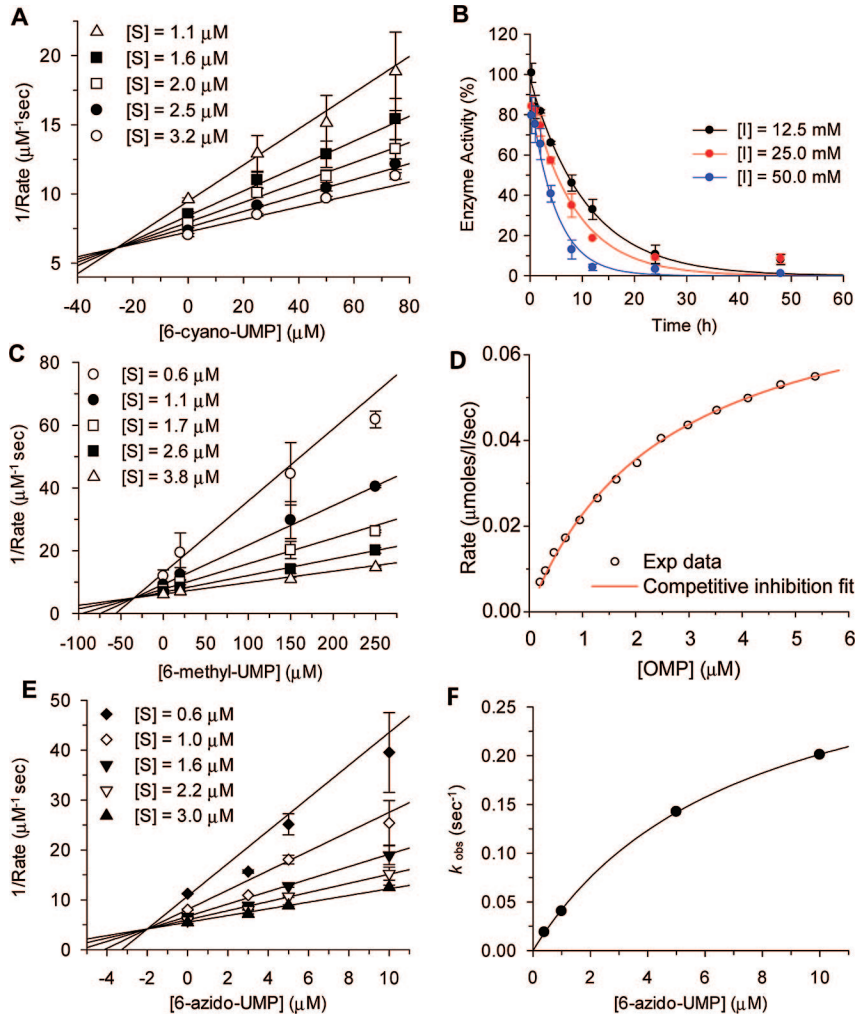

Figure 3. Kinetics profiles of *Pf* ODCase when challenged with 6-CN-UMP, 6-methyl-UMP, 6-amino-UMP, and 6-azido-UMP (**6**, **16**, **15**, and **14**, respectively). (A) Dixon plot for the competitive inhibition of *Pf* ODCase by 6-cyano-UMP (**6**). (B) Time-dependent inhibition of *Pf* ODCase by 6-cyano-UMP (**6**). (C) Competitive inhibition of *Pf* ODCase by 6-methyl-UMP (**16**). (D) Nonlinear least-squares fit of the raw data for the competitive inhibition of *Pf* ODCase by 6-amino-UMP (**15**). (E) Competitive inhibition of *Pf* ODCase by 6-azido-UMP (**14**). (F) Nonlinear least-squares fit of the k_{obs} vs [*I*] for the inhibition of *Pf* ODCase by 6-azido-UMP (**14**).

although we could not chemically synthesize the mononucleotides of **12** and **13**.

When the 6-methyl group was present on the pyrimidine of UMP, a hydrophobic pocket formed by the residues Tyr149, Thr163, Val164, Ile166, and Leu191 and adjacent to the critical catalytic residues was occupied by this small hydrophobic group (Figure 2A). This provided a reasonable explanation for the moderate inhibition of *Pf* ODCase by 6-methyl-UMP (**16**). Similarly, 6-methylamino and 6-dimethylamino moieties could easily be accommodated into

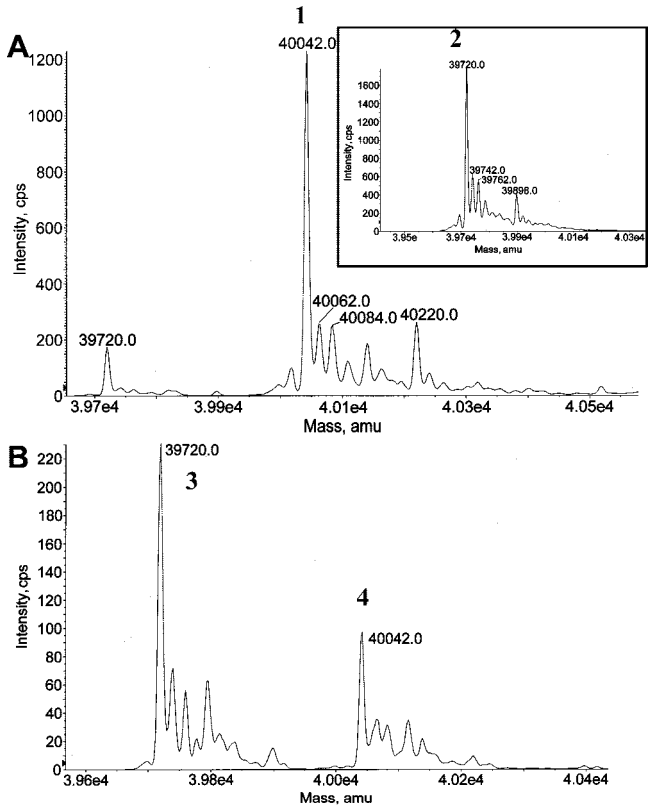

Figure 4. Mass spectral analyses of the complexes of *Pf* ODCase with 6-iodo-UMP, **7** (panel A), and with 6-azido-UMP **14** (panel B) after 72 h incubation at room temperature. A shift in the peak of *Pf* ODCase from 39720.0 daltons to 40042.0 daltons (peaks 2 and 1, panel A) is due to the formation of the *Pf* ODCase covalent complex with inhibitor **7** but without the iodo moiety and the loss of a proton (322.0 daltons). Inset in panel A shows the mass spectrum for *Pf* ODCase alone, as a control experiment (Peak 2). Panel B shows peak 3 (39720.0 daltons) that corresponds to uncomplexed *Pf* ODCase and peak 4 (40042.0 daltons) representing the covalent complex between *Pf* ODCase and **14** but without the azido moiety and an additional proton.

Table 3. Antimalarial Activities of C6-Substituted Uridine Derivatives against *P. falciparum* (3D7) and their Toxicity in CHO Cells

cmpd	*Pf* (3D7) (μM)	CHO cells (μM)
6-iodo-uridine (ref *26*)	6.2 ± 0.7	366 ± 45
6-CN-uridine (**8**)	446 ± 35	>1500
6-N_3-uridine (**9**)	1226 ± 161	>1500
6-NH_2-uridine (**10**)	>1500	>1500
6-Me-uridine (**11**)	530.5 ± 0.1	>1162
6-NHMe-uridine (**12**)	28.5 ± 8.9	71.9 ± 5.3
6-N(Me)$_2$-uridine (**13**)	31.7 ± 10.0	68.3 ± 11.4

this region (Figure 2B). The moderate binding potencies of these compounds may be the result of balancing moderate entropic gains generated by accommodating hydrophobic C6-ligands in a hydrophobic pocket and the loss of binding interactions with the polar/ionic catalytic residues. However, these entropic gains may be important for efficient inhibition of the enzyme activity when a sufficiently high concentration of the inhibitor is present (vide infra).

The nucleoside derivatives **9–13** were evaluated for their antimalarial activities against the cultures of *P. falciparum* 3D7, as well as for their cellular toxicities using the Chinese Hamster Ovary (CHO) cells (Table 3). 6-*N*-Methylamino uridine and 6-*N*,*N*-dimethylamino uridine (**12** and **13**, respectively) exhibited moderate antiplasmodial effects with an IC_{50} of 28 ± 9 and 32 ± 10 μM, respectively. Compound **11** carrying the 6-methyl moiety exhibited a very weak activity against the *P. falciparum* 3D7 isolate, with an IC_{50} of 530.5 ± 0.1 μM. None of the other compounds exhibited significant activity, including 6-azido-uridine (**9**). 6-Iodo-uridine 5′-monophosphate, which is the most potent covalent inhibitor of *Pf* ODCase, exhibited inhibition of several strains of *P. falciparum* (L. Kotra and K. Kain, unpublished results).[26] This is in distinct contrast to what was found with 6-azido-uridine, which, despite the fast covalent inhibition of ODCase by its mononucleotide derivative, did not show any activity against *Plasmodia* cultures. The most probable explanation for this somewhat surprising result is that compound **9**, unlike 6-iodo-uridine, is not effectively phosphorylated by cellular kinases. All nucleoside derivatives **9–13** were also evaluated for their cellular toxicities. Compound **11** was well tolerated by the CHO cells in the toxicity assays, and the IC_{50} was more than 1162 μM. Compounds **12** and **13** inhibited CHO cells with IC_{50}s in the range of 68–72 μM, a value only about 3-fold higher than the concentrations required for the inhibition of *P. falciparum* cultures. The monophosphate derivatives **6** and **14–16** were not evaluated for their antimalarial activities in cell-based assays because these compounds are highly polar mononucleotides.

In summary, 6-azido, 6-amino, 6-methyl, 6-*N*-methylamino, and 6-*N*,*N*-dimethylamino derivatives of uridine were synthesized and evaluated for their activity against the *P. falciparum* pathogen. In addition, the inhibitory potential of several of the corresponding mononucleotides against their enzymic target, ODCase, was measured. UMP derivatives exhibited moderate to potent inhibitory activities against *Pf* ODCase, including the covalent inhibition of ODCase by 6-azido-UMP (**14**). Specifically, 6-*N*-methylamino and 6-*N*,*N*-dimethylamino uridine derivatives (**12** and **13**, respectively) exhibited moderate activities against the *Pf* 3D7 pathogen. For these latter compounds, however, moderate toxicities were also observed in a CHO cell assay, but compound **11** exhibited low toxicity in the same system. Interactions of various C6-substituted UMP derivatives with *Pf* ODCase indicated that both polar and hydrophobic groups can be accommodated at the C6 position of the aromatic ring of mononucleotide inhibitor molecules tightly bound in the active site of ODCase. However, monophosphorylation of the nucleoside derivatives in cell-based assays was unpredictable, thus, the cellular activities of these nucleoside derivatives may not necessarily reflect the inhibition patterns of ODCase by the corresponding mononucleotides. This particular observation is not unique to ODCase nucleoside inhibitors. Various anticancer and antiviral nucleoside inhibitors were subjects of similar limitations.[37] Thus, the investigation of new ODCase inhibitors as antiplasmodial compounds using structure-based design should be complemented with cell-based assays for optimal drug design.

Acknowledgment. The authors thank Ms. Wing Lau for help with the expression and purification of ODCase enzymes and Professor David Clarke for generously allowing the use of the ITC instrument. The authors thank Dr. Junquan Wang for the synthesis of 6-methyl-uridine. This work was supported by grants from the Canadian Institutes of Health Research (E.F.P. and L.P.K.), a CIHR Team Grant in Malaria (K.C.K.), an operating grant MT-13721 (K.C.K.), Genome Canada (K.C.K.), and the Canadian Genetics Disease Network (CGDN; K.C.K.), PSI (K.C.K.). L.P.K. is a recipient of an Rx and D HRF-CIHR research career award. An infrastructure grant from the Ontario Innovation Trust provides support for the Molecular Design and Information Technology Centre (MDIT). E.F.P. and K.C.K.

acknowledge support through the Canada Research Chairs program. We thank the staff at BioCARS, sector 14 beamlines at the Advanced Photon Source, Argonne National Laboratories, for their generous time commitments and support. Use of the Advanced Photon Source was supported by the Basic Energy Sciences, Office of Science, United States Department of Energy, under Contract W-31-109-Eng-38. Use of the BioCARS sector 14 was supported by the National Center for Research Resources, National Institutes of Health, under Grant RR07707. We also gratefully acknowledge the help we received from the staff of the Canadian Macromolecular Crystallography Facility, at the Canadian Light Source, which is supported by NSERC, NRC, CIHR, and the University of Saskatchewan.

Supporting Information Available: Details of HPLC purity data on compounds **11**–**14**. This material is available free of charge via the Internet at http://pubs.acs.org.

References

(1) Biagini, G. A.; O'Neill, P. M.; Bray, P. G.; Ward, S. A. Current drug development portfolio for antimalarial therapies. *Curr. Opin. Pharmacol.* **2005**, *5*, 473–478.
(2) Cunha-Rodrigues, M.; Prudencio, M.; Mota, M. M.; Haas, W. Antimalarial drugs—host target (re)visited. *Biotechnol. J.* **2006**, *1*, 321–332.
(3) Rathore, D.; McCutchan, T. F.; Sullivan, M.; Kumar, S. Antimalarial drugs: Current status and new developments. *Expert Opin. Invest. Drugs* **2005**, *14*, 871–883.
(4) Linares, G. E.; Rodriguez, J. B. Current status and progresses made in malaria chemotherapy. *Curr. Med. Chem.* **2007**, *14*, 289–314.
(5) Bathurst, I.; Hentschel, C. Medicines for malaria venture: Sustaining antimalarial drug development. *Trends Parasitol.* **2006**, *22*, 301–307.
(6) Vangapandu, S.; Jain, M.; Kaur, K.; Patil, P.; Patel, S. R.; Jain, R. Recent advances in antimalarial drug development. *Med. Chem. Rev.* **2007**, *27*, 65–107.
(7) Gero, A. M.; O'Sullivan, W. J. Purines and pyrimidines in malarial parasites. *Blood Cells* **1990**, *16*, 467–484.
(8) Gardner, M. J.; Hall, N.; Fung, E.; White, O.; Berriman, M.; Hyman, R. W.; Carlton, J. M.; Pain, A.; Nelson, K. E.; Bowman, S.; Paulsen, I. T.; James, K.; Eisen, J. A.; Rutherford, K.; Salzberg, S. L.; Craig, A.; Kyes, S.; Chan, M. S.; Nene, V.; Shallom, S. J.; Suh, B.; Peterson, J.; Angiuoli, S.; Pertea, M.; Allen, J.; Selengut, J.; Haft, D.; Mather, M. W.; Vaidya, A. B.; Martin, D. M.; Fairlamb, A. H.; Fraunholz, M. J.; Roos, D. S.; Ralph, S. A.; McFadden, G. I.; Cummings, L. M.; Subramanian, G. M.; Mungall, C.; Venter, J. C.; Carucci, D. J.; Hoffman, S. L.; Newbold, C.; Davis, R. W.; Fraser, C. M.; Barrell, B. Genome sequence of the human malaria parasite *Plasmodium falciparum*. *Nature* **2002**, *419*, 498–511.
(9) Pink, R.; Hudson, A.; Mouries, M. A.; Bendig, M. Opportunities and challenges in antiparasitic drug discovery. *Nat. Rev. Drug Discovery* **2005**, *4*, 727–740.
(10) Jones, M. E. Pyrimidine nucleotide biosynthesis in animals: Genes, enzymes, and regulation of UMP biosynthesis. *Annu. Rev. Biochem.* **1980**, *49*, 253–279.
(11) Mehta, S. R.; Das, S. Management of malaria: Recent trends. *J. Commun. Dis.* **2006**, *38*, 130–138.
(12) Kremsner, P. G.; Krishna, S. Antimalarial combinations. *Lancet* **2004**, *364*, 285–294.
(13) Nwaka, S.; Hudson, A. Innovative lead discovery strategies for tropical diseases. *Nat. Rev. Drug Discovery* **2006**, *5*, 941–955.
(14) Jana, S.; Paliwal, J. Novel molecular targets for antimalarial chemotherapy. *Int. J. Antimicrob. Agents* **2007**, *30*, 4–10.
(15) Biagini, G. A.; O'Neill, P. M. O.; Bray, P. G.; Ward, S. A. Current drug development portfolio for antimalarial therapies. *Curr. Opin. Pharmacol.* **2005**, *5*, 473–478.
(16) Miller, B. G.; Wolfenden, R. Catalytic proficiency: The unusual case of OMP decarboxylase. *Annu. Rev. Biochem.* **2002**, *71*, 847–885.
(17) Sievers, A.; Wolfenden, R. Equilibrium of formation of the 6-carbanion of UMP, a potential intermediate in the action of OMP decarboxylase. *J. Am. Chem. Soc.* **2002**, *124*, 13986–13987.
(18) Snider, M. J.; Wolfenden, R. The rate of spontaneous decarboxylation of amino acids. *J. Am. Chem. Soc.* **2000**, *122*, 11507–11508.
(19) Seymour, K. K.; Lyons, S. D.; Phillips, L.; Rieckmann, K. H.; Christopherson, R. I. Cytotoxic effects of inhibitors of de novo pyrimidine biosynthesis upon *Plasmodium falciparum*. *Biochemistry* **1994**, *33*, 5268–5274.
(20) Christopherson, R. I.; Lyons, S. D.; Wilson, P. K. Inhibitors of de novo nucleotide biosynthesis as drugs. *Acc. Chem. Res.* **2002**, *35*, 961–971.
(21) Krungkrai, J.; Krungkrai, S. R.; Phakanont, K. Antimalarial activity of orotate analogs that inhibit dihydroorotase and dihydroorotate dehydrogenase. *Biochem. Pharmacol.* **1992**, *43*, 1295–1301.
(22) Scott, H. V.; Gero, A. M.; O'Sullivan, W. J. In vitro inhibition of *Plasmodium falciparum* by Pyrazofurin, an inhibitor of pyrimidine biosynthesis de novo. *Mol. Biochem. Parasitol.* **1986**, *18*, 3–15.
(23) Fujihashi, M.; Bello, A. M.; Poduch, E.; Wei, L.; Annedi, S. C.; Pai, E. F.; Kotra, L. P. An unprecedented twist to ODCase catalytic activity. *J. Am. Chem. Soc.* **2005**, *127*, 15048–15050.
(24) Poduch, E.; Bello, A. M.; Tang, S.; Fujihashi, M.; Pai, E. F.; Kotra, L. P. Design of inhibitors of orotidine monophosphate decarboxylase using bioisosteric replacement and determination of inhibition kinetics. *J. Med. Chem.* **2006**, *49*, 4937–4945.
(25) Kotra, L. P.; Pai, E. F.; Bello, A. M.; Fujihashi, M.; Poduch, E. Inhibitors of orotidine monophosphate decarboxylase (ODCase) activity. U.S. Patent Application 60/596,537, 2005,patent pending.
(26) Bello, A. M.; Poduch, E.; Fujihashi, M.; Amani, M.; Li, Y.; Crandall, I.; Hui, R.; Lee, P. I.; Kain, K. C.; Pai, E. F.; Kotra, L. P. A potent, covalent inhibitor of orotidine 5′-monophosphate decarboxylase with antimalarial activity. *J. Med. Chem.* **2007**, *50* (5), 915–921.
(27) Wu, N.; Mo, Y.; Gao, J.; Pai, E. F. Electrostatic stress in catalysis: structure and mechanism of the enzyme orotidine monophosphate decarboxylase. *Proc. Natl. Acad. Sci. U.S.A.* **2000**, *97*, 2017–2022.
(28) Dixon, M. The graphical determination of K_m and K_i. *Biochem. J.* **1972**, *129*, 197–202.
(29) Trager, W.; Jensen, J. Human malaria parasites in continuos culture. *Science* **1976**, *193*, 673–675.
(30) Smilkstein, M.; Sriwilaijaroen, N.; Kelly, J. X.; Wilairat, P.; Riscoe, M. Simple and inexpensive fluorescence-based technique for high-throughput antimalarial drug screening. *Antimicrob. Agents Chemother.* **2004**, *48*, 1803–1806.
(31) Campling, B. G.; Pym, J.; Galbraith, P. R.; Cole, S. P. Use of MTT assay for rapid determination of chemosensitivity of human leukemic blast cells. *Leuk. Res.* **1988**, *12*, 823–831.
(32) Otwinowski, Z.; Minor, W. Processing of X-ray diffraction data collected in oscillation mode. *Methods Enzymol.* **1997**, *276*, 307–326.
(33) Vagin, A.; Teplyakov, A. MOLREP: An automated program for molecular replacement. *J. Appl. Crystallogr.* **1997**, *30*, 1022–1025.
(34) Murshudov, G. N.; Vagin, A. A.; Dodson, E. J. Refinement of macromolecular structures by the maximum-likehood method. *Acta Crystallogr.* **1997**, *D53*, 240–255.
(35) Emsley, P.; Cowtan, K. Model building tools for molecular graphics. *Acta Crystallogr.* **2004**, *D60*, 2126–2132.
(36) *SYBYL 7.0*, Tripos Inc.: 1699 South Hanley Rd., St. Louis, Missouri, 63144.
(37) Tan, X.; Chu, C. K.; Boudinot, F. D. Development and optimization of anti-HIV nucleoside analogs and prodrugs: A review of their cellular pharmacology, structure−activity relationships, and pharmacokinetics. *Adv. Drug Delivery Rev.* **1999**, *39*, 117–151.

JM7010673